analytical chemistry

Article

Cite This: Anal. Chem. 2017, 89, 13494−13501

pubs.acs.org/ac

Structural and Functional Characterization of a Hole−Hole Homodimer Variant in a "Knob-Into-Hole" Bispecific Antibody

Hui-Min Zhang,*[,†] Charlene Li,[†] Ming Lei,[†] Victor Lundin,[†] Ho Young Lee,[‡] Milady Ninonuevo,[†] Kevin Lin,[§] Guanghui Han,[∥] Wendy Sandoval,[∥] Dongsheng Lei,[⊥] Gang Ren,[⊥] Jennifer Zhang,[†] and Hongbin Liu*[,†,○]

[†]Protein Analytical Chemistry, [‡]Biological Technologies, [§]Analytical Operations, and [∥]Departments of Microchemistry, Proteomics and Lipidomics, Genentech Inc., 1 DNA Way, South San Francisco, California 94080, United States

[⊥]The Molecular Foundry, Lawrence Berkeley National Laboratory, One Cyclotron Road, Berkeley, California 94720, United States

Supporting Information

ABSTRACT: Bispecific antibodies have great potential to be the next-generation biotherapeutics due to their ability to simultaneously recognize two different targets. Compared to conventional monoclonal antibodies, knob-into-hole bispecific antibodies face unique challenges in production and characterization due to the increase in variant possibilities, such as homodimerization in covalent and noncovalent forms. In this study, a storage- and pH-sensitive hydrophobic interaction chromatography (HIC) profile change was observed for the hole−hole homodimer, and the multiple HIC peaks were explored and shown to be conformational isomers. We combined traditional analytical methods with hydrogen/deuterium exchange mass spectrometry (HDX MS), native mass spectrometry, and negative-staining electron microscopy to comprehensively characterize the hole−hole homodimer. HDX MS revealed conformational changes at the resolution of a few amino acids overlapping the C_H2-C_H3 domain interface. Conformational heterogeneity was also assessed by HDX MS isotopic distribution. The hole−hole homodimer was demonstrated to adopt a more homogeneous conformational distribution during storage. This conformational change is likely caused by a lack of C_H3 domain dimerization (due to the three "hole" point mutations), resulting in a unique storage- and pH-dependent conformational destabilization and refolding of the hole−hole homodimer Fc. Compared with the hole−hole homodimer under different storage conditions, the bispecific heterodimer, guided by the knob-into-hole assembly, proved to be a stable conformation with homogeneous distribution, confirming its high quality as a desired therapeutic. Functional studies by antigen binding and neonatal Fc receptor (FcRn) binding correlated very well with the structural characterization. Comprehensive interpretation of the results has provided a better understanding of both the homodimer variant and the bispecific molecule.

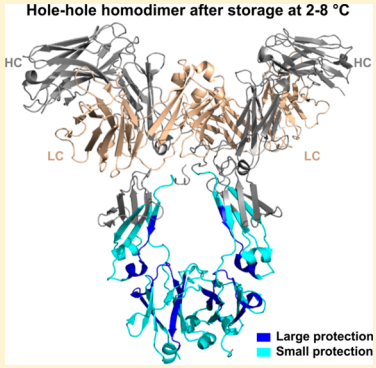

Bispecific antibodies (BsAbs) have gained significant interest in the biotech field as therapeutic alternatives to conventional monoclonal antibodies (mAbs).[1−3] Currently, more than 60 BsAb formats exist,[1,3] and they can be differentiated into two major classes: with or without an Fc region.[4] The BsAbs with an Fc region are more popular because of their known stability and long half-life due to their large size and neonatal Fc receptor (FcRn)-mediated recycling process.[4,5] The fermentation and purification processes established for the production of standard IgG molecules can often be leveraged for such BsAbs. Different from conventional mAbs, which have two identical antigen-recognizing or Fab moieties, BsAbs have two different paratopes on the variable domains recognizing two different antigens. This unique feature results in more complex variants for BsAbs, for example, homodimers from the two different arms, mispairing of light chains, and so on. To produce BsAbs, the "knob-into-hole" format has been adopted to promote heavy-chain heterodimerization of the two half antibodies.[6,7] The knob (T366W) and hole (T366S, L368A, and Y407 V) mutants are located at the C_H3 domain interface, and thus should not impact antigen binding or Fc function. The light chain mispairing problem can be overcome during production by several approaches.[3] One approach is through an in vitro assembly step, where two half antibodies are expressed in two different host cells. After two separate Protein A affinity capture steps, the two half antibodies are mixed for in vitro assembly by reduction and oxidation[8] followed by downstream purification of the BsAb.

The knob-into-hole design and in vitro assembly can efficiently drive heterodimerization of the heavy chains; however, some level of homodimers (including knob−knob homodimers and hole−hole homodimers) are still present during half antibody purification and BsAb assembly.[7] In fact, homodimers are the typical minor forms in the affinity-captured pools of each arm. It is challenging to separate the homodimers

Received: September 19, 2017
Accepted: November 12, 2017
Published: November 12, 2017

DOI: 10.1021/acs.analchem.7b03830
Anal. Chem. 2017, 89, 13494−13501

from the BsAbs and quantify their levels, depending on the physicochemical property differences between the two arms. The homodimer variants also have different forms, for example, covalent or noncovalent forms.[9] Elliott et al. discovered the molecular details for knob-into-hole and homodimer interactions in the Fc of an IgG1 BsAb.[10] They solved X-ray crystal structures of both the knob−knob and hole−hole Fc fragment homodimers, which revealed an antiparallel Fc orientation. Intact mass analysis has also been used for bispecific variants identification and quantitation.[9,11,12]

Homodimers can potentially cause undesired bioactivity. In addition, because of their potentially unnatural structure and presumed low stability, the homodimers may be more prone to aggregate which may lead to increased immunogenicity.[11] Detailed characterization and close monitoring of the homodimers during the production process are crucial to develop safe and efficacious BsAbs.

When typical biophysical and analytical methods used for conventional mAbs are applied to characterize BsAbs, it is very challenging to successfully separate and monitor the homodimers. There is increasing interest in using high-resolution structural methods to characterize mAbs. As is typical for IgG, there is no full-length BsAb X-ray structure available, and only the Fc of a BsAb has been solved.[10,13] By monitoring the dynamics of backbone amide hydrogen exchange into deuterium, hydrogen−deuterium exchange mass spectrometry (HDX MS) can probe protein dynamics and conformational change in solution. In recent years, HDX MS has been widely used to characterize protein conformation and protein−protein interactions,[14−17] for example, epitope mapping,[18] conformational change due to chemical modifications,[19,20] or aggregation mechanism analysis.[21,22] The interaction of IgG with its purification resin protein A and the pH-dependent interaction with FcRn have also been reported.[22,23] Pan et al. discussed the conformational impact of drug conjugation on the mAb.[24]

In this study, a slow change during storage at 2−8 °C was observed by hydrophobic interaction chromatography (HIC) for the hole−hole homodimer variant of a knob-into-hole BsAb (BsAb1). No chemical modifications were detected during storage, indicating that the HIC peaks are multiple conformational isomers for this variant. The different conformational isoforms and their changing profile during storage are of concern not only for its quantitation and control, but also for its potential bioactivity and immunogenicity risks in a therapeutic context. We combined traditional methods, such as HIC, size exclusion chromatography (SEC), and liquid chromatography−mass spectrometry (LC-MS), with state-of-the-art methods, for example, native MS, HDX MS, and electron microscopy (EM)[25] to characterize the conformations of the knob-into-hole BsAb and the hole−hole homodimer during storage. The conformational changes identified by HDX MS were mapped to an IgG1 structural model for the hole−hole homodimer variant, and the results were consistent with all other experimental observations, including antigen binding and FcRn binding data. To our knowledge, this is the first demonstration of HDX's ability to detect the structural change of a molecule without any primary structural change (chemical modifications) or matrix change, since no binding partners were present and pH stayed constant at around 5.8 during storage at 2−8 °C. This approach has helped us better understand the root cause of its structural change and better control this unique type of BsAb impurity.

EXPERIMENTAL SECTION

Production of the Hole−Hole Homodimer for BsAb1. The hole−hole homodimer of BsAb1, which is an in vitro assembled knob-into-hole BsAb, was produced and purified at Genentech Inc. (South San Francisco, CA). The harvested cell culture fluid of the hole half antibody was purified through protein-A affinity chromatography. The pH of the protein-A pool was adjusted from 3.3 to 5.0, and Poros cation exchange chromatography (CEX) was used to separate the hole−hole homodimer from the half antibody and other species. The elution pH was 5.5. Ultrafiltration/diafiltration was applied and conditioned at pH 5.8 in 20 mM histidine acetate formulation buffer. The resulting hole−hole homodimer was kept at −70 °C for storage. The identity of the isolated hole−hole homodimer and the knob-into-hole bispecific heterodimer were confirmed by intact mass analysis, which also confirmed that the hole−hole homodimer was a covalent homodimer.

Hydrophobic Interaction Chromatography. HIC was performed on a Waters Alliance 2695 HPLC (Waters Corporation, Millford, MA) with a Dionex ProPac HIC-10 column, 4.6 × 100 mm (Thermo Scientific, Waltham, MA). Mobile phase A was 20 mM Tris buffer (pH 7.5) containing 1.5 M ammonium sulfate. Mobile phase B was 20 mM Tris buffer (pH 7.5). Each sample was diluted to 2 mg/mL with LC-grade water. The protein load for each injection was 40 μg. A linear gradient from 0 to 100% mobile phase B in 60 min was used. The column temperature was maintained at 25 °C, and the flow rate was 0.8 mL/min. The column effluent was monitored at 280 nm.

Intact Mass Analysis by Native Mass Spectrometry. Native MS analysis with an Exactive Plus extended mass range (EMR) Orbitrap mass spectrometer was used to study the charge-state distribution of the hole−hole homodimers. A brief description of the method is provided in the Supporting Information.

Hydrogen/Deuterium Exchange Mass Spectrometry. The HDX MS experiments of hole−hole homodimers stored at −70 °C and 2−8 °C for 9 months were performed on a fully automated Leap robotic system (Leap Technologies, Carr, NC) connected to an Orbitrap Elite mass spectrometer (Thermo Scientific). The two samples were at 5 mg/mL in 20 mM sodium acetate buffer (pH 5.3 ± 0.3) in H_2O. The same sodium acetate buffer was also prepared in D_2O for deuterium labeling, pD 5.3 ± 0.3.

For deuterium labeling, 3.5 μL of the hole−hole homodimer sample was mixed with 55 μL of the labeling buffer in D_2O stored at both −70 °C and 2−8 °C. The samples were labeled for 30 s, 1 min, 10 min, 1 h, and 4 h in D_2O buffers at 20 °C in triplicate, and quenched with 55 μL of quench solution (8 M urea, 1 M TCEP·HCl, pH 2.2). Immobilized protease XIII/pepsin (1:1) column (2.0 × 30 mm; NovaBioAssays, Inc., Woburn, MA) was used for online digestion in 0.1% formic acid and 0.04% TFA in H_2O (pH 2.3), at 100 μL/min. The digests were captured on a trapping column (Waters ACQUITY BEH C18 VanGuard Precolumn 2.1 × 5 mm) and then eluted to a Waters BEH C_{18} UHPLC column (2.1 × 50 mm) for peptide separation on a Waters Nano Acquity HPLC system. A 12 min gradient of 5−50% B (A/B: 0.1% formic acid and 0.05% TFA in H_2O/acetonitrile) was used, at 50 μL/min. The eluted peptides were directed into an Orbitrap mass spectrometer with electrospray ionization for detection, in the m/z range 300−1800 at a resolving power of 60000 at m/z

DOI: 10.1021/acs.analchem.7b03830
Anal. Chem. 2017, 89, 13494−13501

400. Peptides were identified using a combination of exact mass and MS/MS aided by Mascot search. Peptide deuterium levels were determined using EXMS[26] and a python script.[27] The average relative deuterium uptake difference (ARDD)[18] for all the time points was also automatically calculated by the modified python script to represent the overall protection on each peptide.

Antibody Structure by Electron Microscopy and Antigen Binding. Negative-staining electron microscopy (NS EM) using an optimized negative-staining (OpNS) protocol was used to study the structure of the antibody homodimers. Hole-hole homodimer binding with the antigen peptide was measured using an antigen binding assay. Brief descriptions of these methods are provided in the Supporting Information.

RESULTS AND DISCUSSION

Different Conformational Isoforms Detected for the Hole−Hole Homodimer. In an attempt to monitor and quantify the knob−knob and hole−hole homodimers in the knob-into-hole bispecific product, a HIC method was developed. Unlike the bispecific heterodimer, which has a single HIC peak, the hole−hole homodimer displayed three major peaks when analyzed after being thawed from −70 °C (Figure 1A).

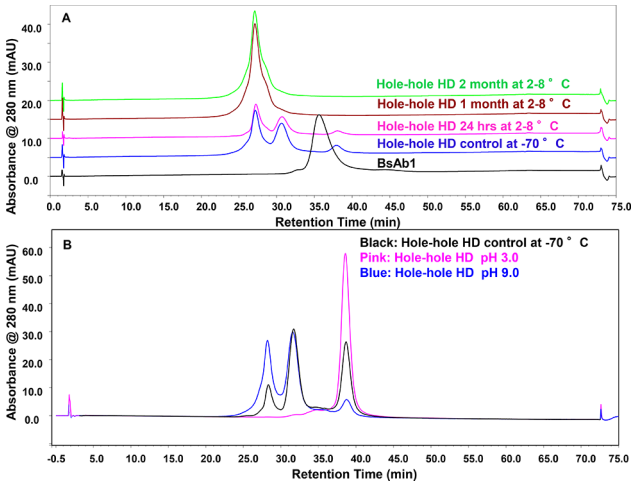

Figure 1. HIC profile of BsAb1 and the hole−hole homodimer (HD) (A) at different storage conditions; (B) hole−hole HD frozen control, buffer exchanged to pH 3.0 and pH 9.0, respectively. Note: The −70 °C control materials used in this figure were from different batches and formulated in different buffer conditions including pH [pH 5.8 for (A) and pH 5.5 for (B)]. Their HIC profiles served as the internal reference within the same experiment only.

Intact mass analysis by a chip-TOF technique[9] for the isolated HIC peaks revealed protein species with the same masses, suggesting that the multiple HIC peaks represented conformational isomers. Peptide mapping analysis did not identify any significant increase in chemical modifications, with only a trace level (<0.5%) of Met 254 and Met 430 oxidation detected in the −70 °C or the 2−8 °C sample. The lack of dissociation between heavy chains during chip-TOF-MS analysis (under denaturing condition) suggests that the homodimer in question is covalently linked. The discovery of multiple conformations of the hole−hole homodimer was surprising and prompted further study upon storage.

The HIC profile of the hole−hole homodimer had shifted to the left upon storage at 2−8 °C for 1 month at pH 5.8 (Figure 1A), indicating that the hydrophobicity slowly decreases. This conformational change was slow, because after 24 h at 2−8 °C, the profile showed little change. Subsequent experiments revealed that the HIC profile was also pH-dependent. Figure 1B shows that immediately after the hole−hole homodimer was buffer exchanged from pH 5.8 to pH 3.0, it appears as a single peak eluting at the far right side of the chromatogram (more hydrophobic). However, for the same pH 5.8 starting material, after buffer exchange to pH 9.0, the HIC profile shifts to the left (less hydrophobic). Similar to storage at 2−8 °C, the basic pH caused a decrease in the hydrophobicity of the sample. The BsAb1, however, did not show any such storage- or pH-dependent change on the HIC profile; instead, it stayed as a single peak eluting at the same position (data not shown).

To confirm the slow profile change from high to low hydrophobicity, the hole−hole homodimer was buffer exchanged to pH 3.0 and then to pH 7.5, followed by HIC analysis at different time points after storage at 2−8 °C. The pH change from pH 3.0 to pH 7.5 caused a peak with lower hydrophobicity on the left side of the HIC profile to increase (see Supporting Information, Figure S-1). However, even after 18 h at 2−8 °C, the majority of the molecules stayed on the right side and only a small portion of the homodimer shifted to the left, demonstrating that the conformational change is slow.

SEC analysis was also performed, as described in the Supporting Information, to assess the hydrodynamic radius (R_h) of the hole−hole homodimer samples. The early eluting species have a larger R_h than the late-eluting species, which indirectly relates to the conformational change of the sample. Figure S-2 (see Supporting Information) displays the SEC data for the control sample (stored at −70 °C) and the samples stored at 2−8 °C for 2 weeks and 6 months. All three samples eluted as monomer, indicating that the multiple species observed in the HIC profile (Figure 1) represent the homodimer monomer, not high molecular weight aggregate.

The sample stored at −70 °C displayed two species shown as two split peaks (Figure S-2), present in about equal abundance. The two-week sample has a higher abundance of the species that elutes later, and the six-month sample has mainly one species that elutes later. The right-shifting SEC profile clearly indicates that the R_h of the hole−hole homodimer continues to decrease after storing at 2−8 °C from 2 weeks to 6 months. Since the molecular weight stays the same, the R_h change can perhaps only be explained by conformational change, indicating that upon storage at 2−8 °C, the protein begins to take on a more compact conformation.

Structural Basis for the Conformational Isoforms from Native MS. Since these HIC-separated peaks were most likely conformational isomers of the hole−hole homodimer, we wanted to further characterize their structures. The charge-state distribution by native MS can be related to the folding of a protein, where a lower charge distribution generally means a more folded and compact structure.[28] Samples in native buffer (in 100 mM ammonium acetate, pH 6.8) were infused onto a mass spectrometer to compare the conformational difference of the hole−hole homodimers stored at the two conditions (Figure 2, upper panel, −70 °C; lower panel, 2−8 °C for 6 months). Compared with the sample stored at −70 °C, the sample stored at 2−8 °C has a higher m/z distribution and lower charge states, indicating less solvent-exposed surface area. Clearly, the −70 °C sample displayed two Gaussian

DOI: 10.1021/acs.analchem.7b03830
Anal. Chem. 2017, 89, 13494−13501

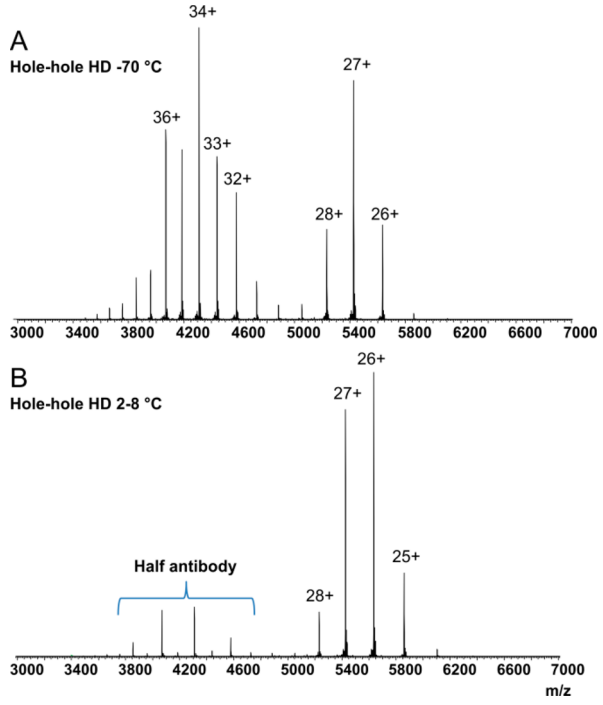

Figure 2. Native MS data for the hole−hole homodimer (HD) stored for 6 months at (A) −70 °C and (B) 2−8 °C.

distributions, indicating two conformational species. The 2−8 °C sample has m/z peaks (3800−4600 range) with twice the spacing as in the −70 °C sample, which corresponded to half antibody masses due to the direct infusion of the samples (no separation between the homodimer and the half antibody). A closer look at the charge states for the −70 °C sample revealed a mixture of homodimer and half antibody, because the relative peak abundance of the 36^+ and 34^+ is greater as compared with a regular Gaussian distribution, indicating two species in the sample.

Hole−Hole Homodimer Becomes More Compact after Storage at 2−8 °C as Confirmed by HDX MS. To obtain high-resolution conformational information by HDX MS, it is essential to get high sequence coverage on the proteins being compared. Protease type XIII is superior to pepsin in terms of generating more overlapping peptides in solution.[29−31] For this study, the column with protease type XIII and pepsin immobilized at 1:1 ratio resulted in the highest sequence coverage and the most number of unique peptides. For the hole−hole homodimer samples stored at −70 °C and 2−8 °C, we acquired 330 unique peptides and achieved high sequence coverage at 94%.

Under exactly the same experimental conditions, deuterium uptake was compared for the hole−hole homodimer samples stored at −70 °C and 2−8 °C for 9 months. As shown in Figure 3A, the peptides in the Fab regions on both the heavy and light chains did not show any difference in deuterium uptake (e.g.,

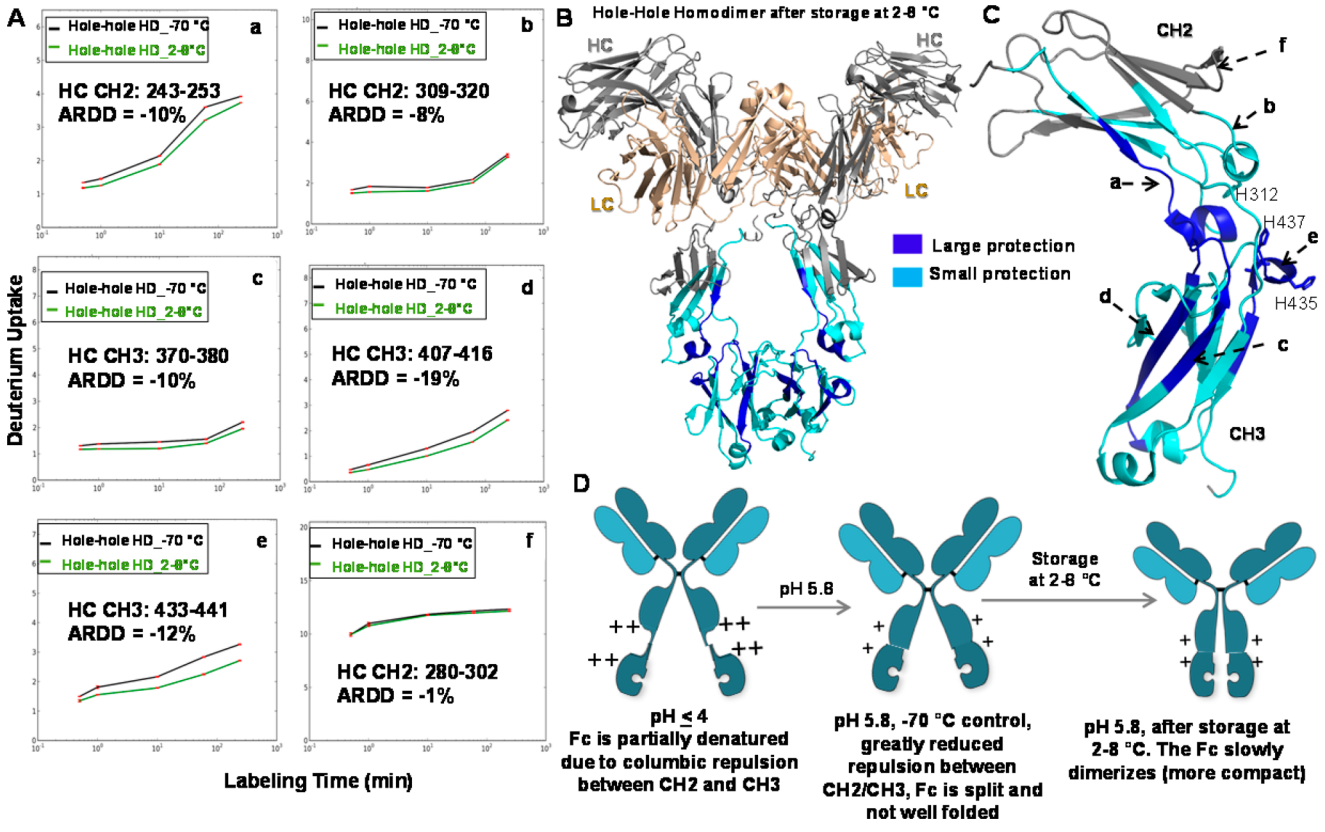

Figure 3. (A) Representative time-course HDX MS data for the hole−hole homodimer (HD) 2−8 °C vs −70 °C; (B) HDX MS results mapped on a human IgG1 mAb, 1HZH; light brown, light chain; gray, heavy chain; blue, large protection (ARDD ≤ −10%); and light blue, a small protection (−10% < ARDD ← 3%); (C) Zoomed-in color-coded HDX MS results on the Fc region of a human IgG1 mAb: 1HZH. The peptides shown in (A) are labeled; (D) Proposed model for the hole−hole HD under different pH and storage conditions. After storage at 2−8 °C or pH increases, the hole−hole HD can slowly form a stable conformation by the Fc dimerization.

DOI: 10.1021/acs.analchem.7b03830
Anal. Chem. 2017, 89, 13494−13501

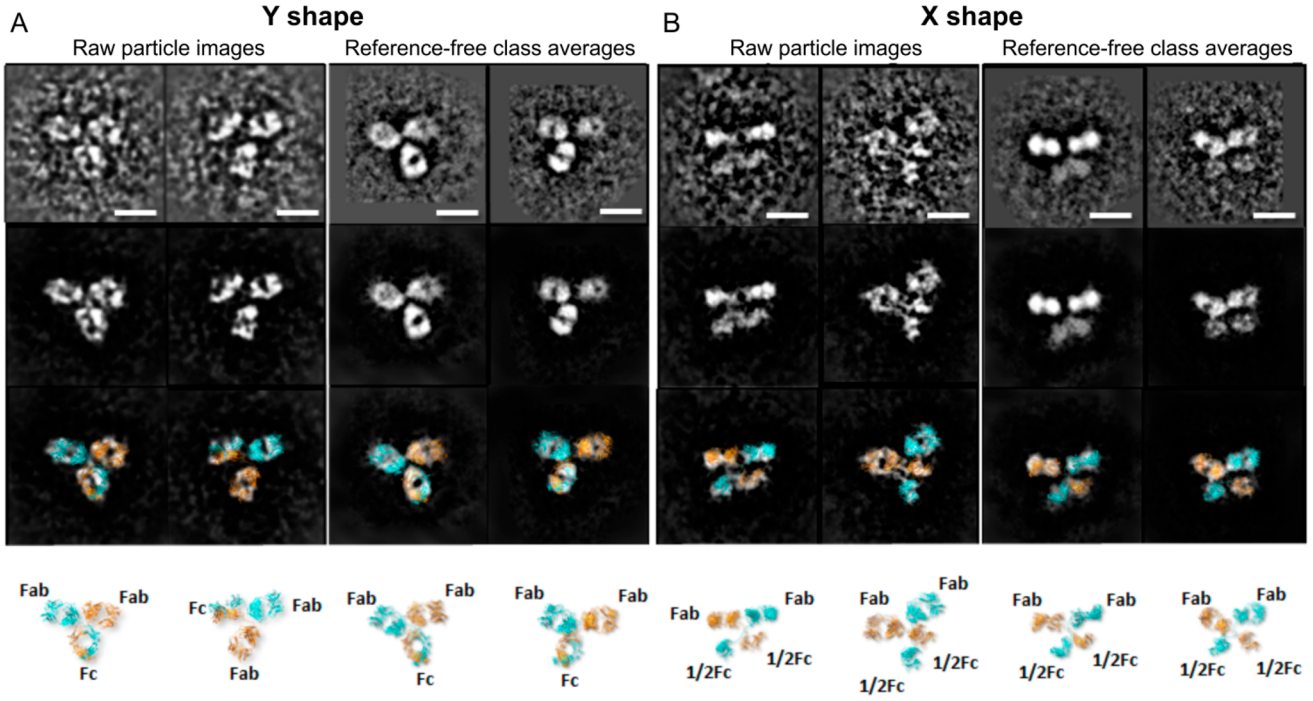

Figure 4. NS EM of the hole−hole homodimer sample stored at −70 °C. Representative single-molecule EM raw images and selected reference-free class averages of (A) the Y- and (B) X-shaped molecules are indicated, with possible domain identification labeled at the bottom. Top row, the raw images of particles and raw class averages; second row, their corresponding images after soft-boundary masking; third row, the models overlapped with the masked images; bottom row, the structure models; scale bars = 10 nm.

HC CDR2 46−70), indicating no conformational difference in the Fab region.

Large regions on the heavy chain Fc region (CH2 and CH3) displayed reduced deuterium uptake in the sample stored at 2−8 °C for 9 months, implying increased structural stability after storage at 2−8 °C. The HDX results are color-coded on a conventional IgG1 molecule (PDB ID: 1HZH, Figure 3B), similar to the hole−hole homodimer. The cold colors (blue and cyan) indicate more protection or less dynamics in the 2−8 °C sample compared with the −70 °C sample. A closer look at the Fc region revealed details of the conformational change after 2−8 °C storage (Figure 3C). On the C_H2 domain, the large protection is located mainly on peptide a (HC 243−253). On the C_H3 domain, the hole mutants T368S and L370A on or near peptide c (HC 370−380), as well as Y409 V on peptide d (HC 407−416) all become protected after 2−8 °C storage. (Note: the numbering is off by two amino acid residues from the generic framework numbering reported in the literature.[7]) These two β-sheets where peptides c and d reside are normally involved in the C_H3 dimer interaction.[6] Peptide e (HC 433−441), with two histidine residues (His435/His437), is also largely protected after storage at 2−8 °C. These high-resolution HDX MS data demonstrated that some regions of the hole−hole homodimer Fc domain slowly fold together and form a more compact structure. These data are consistent with the results showing that after storage at 2−8 °C, the homodimer becomes less hydrophobic by HIC, has smaller R_h by SEC, and bears fewer charges by native MS.

Potential Mechanism for the Conformational Change in the Hole−Hole Homodimer. Since the hole−hole homodimer conformational change is impacted by storage conditions, it is important to understand if the conformation is affected by the manufacturing process. After protein A affinity chromatography, the protein is eluted in pH 3.3 before adjusting to pH 5.0, followed by CEX purification and buffer exchange to pH 5.8. It was previously reported that IgG1 antibodies show reduced structural stability in the Fc domain at low pH of 5.5 due to columbic repulsion from positively charged histidine residues at the junction between the C_H2 and C_H3 domains.[23] It is proposed that under low pH, the protein A-eluting conditions, the hole−hole homodimer (also an IgG1 molecule) is unstable, and the C_H2 and C_H3 domains are disconnected due to columbic repulsion from His312 in C_H2 and His435/His437 in C_H3. The conformational change to a more hydrophobic and less-folded state with low pH (3.0) exposure (Figure 1B) supports this model. When the pH of the solution is increased to 5.8 or higher, most of the histidine residues return to neutral charge, and the columbic repulsion associated with the Fc destabilization at low pH is greatly reduced. However, the refolding of the hole−hole homodimer Fc is slow due to the lack of a stable C_H3-C_H3 domain dimer (as a result of the three "hole" mutations). After prolonged storage at pH 5.8 or higher, the Fc eventually reaches a local minimum energy state, as suggested by the reduced dynamics on both C_H2 and C_H3 domains by HDX MS.

Evidence from Negative-Staining Electron Microscopy Data. To confirm the structural variation at the molecular imaging level, electron microscopy (EM) was used to examine the sample of hole−hole homodimer after storage at −70 °C, as an orthogonal method to validate the proposed structure based on HDX data. Representative NS EM particles' images showed two main morphology categories observed for the hole−hole homodimer, Y- and X-shaped species (Figure 4). To confirm that the observed structures were statistically significant, reference-free class averaging analysis was performed. The selected reference-free class averages confirmed the existence of the Y- and X-shaped species. The Y-shaped species are similar to what is expected for a conventional IgG

DOI: 10.1021/acs.analchem.7b03830
Anal. Chem. 2017, 89, 13494−13501

molecule. However, the X-shaped species was only observed in this hole−hole homodimer sample, but not in conventional IgG or bispecific molecules. The X- and Y-shaped species differ in the Fc region where the two halves are away from each other, implying less interaction between the two halves. The particle images observed by EM are snap-shots of the dynamics of the molecule. Uranyl formate used in OpNS works at a lower pH value (~4.5), which may partially denature the hole−hole homodimer's conformation, as shown on Figure 3D. Because of the low pH (~4.5) of the fixing reagent, a comparison of the hole−hole homodimer samples at different storage conditions, as shown in Figure 3, by HDX MS was not possible by EM, mainly due to the quick conformational change of the hole−hole homodimer at low pH.

Knob-Into-Hole Bispecific Molecule Is the Most Stable Form. The conformation of the desired knob-into-hole BsAb1 was also compared with the hole−hole homodimers by HDX. Three samples (BsAb1 and the hole−hole homodimers at −70 °C and 2−8 °C) were compared (Figure 5A). The BsAb1 exhibits the least deuterium uptake in the Fc region, and it is therefore the most folded and stable form among the three samples. Not surprisingly, the C_H3 domain displayed the highest stability in the BsAb1, consistent with the intended purpose of the knob and hole point mutations to promote knob-into-hole side chain packing. Since the BsAb1 is more stable than the hole−hole homodimers, even after prolonged storage at 2−8C, this implies an inability on the part of the homodimer to form a native Fc conformation.

As expected, no deuterium uptake difference was seen in the complementarity determining regions (CDRs) comparing BsAb1 and the hole−hole homodimers, suggesting little or no impact due to the knob or hole mutations and/or Fc conformation. This high-resolution structural information strongly supports the knob-into-hole bispecific design that the Fab of each half antibody is maintained, without any impact from the other half.

EX1 Kinetics Observed for the Hole−Hole Homodimer Conformational Change. In addition to the processed deuterium incorporation data, HDX MS raw data also provide insight into protein conformation. Two exchange kinetics of HDX MS have been described, EX2 and EX1.[29,32,33] The EX2 exchange pattern usually represents a stable and homogeneous protein population. The EX1 exchange kinetics usually implies a heterogeneous protein population with different protein conformations. In Figure 5B, a C_H2 peptide (243−253) displayed EX1 exchange pattern for the hole−hole homodimer stored at −70 °C; however, the sample stored at 2−8 °C and the BsAb1 followed EX2 exchange kinetics. In addition, other peptides in the C_H2 and C_H3 domains that also exhibited EX1 distribution in the −70 °C hole−hole homodimer include: 309−320, 336−358, 407−428, and 428−448. Therefore, the hole−hole homodimer at −70 °C is a mixture of different populations with different conformations. These conformations can be correlated with the different HIC profiles. The fast exchanging population is likely to be the more hydrophobic peak, and the slow exchanging population is likely to be the least hydrophobic peak. After prolonged storage (9 month) at 2−8 °C, the EX2 pattern suggests that the homodimer becomes one homogeneous species shown as a single low-hydrophobicity peak on the HIC profile (Figure 1A), again implying that it is adopting a stable and homogeneous conformation.

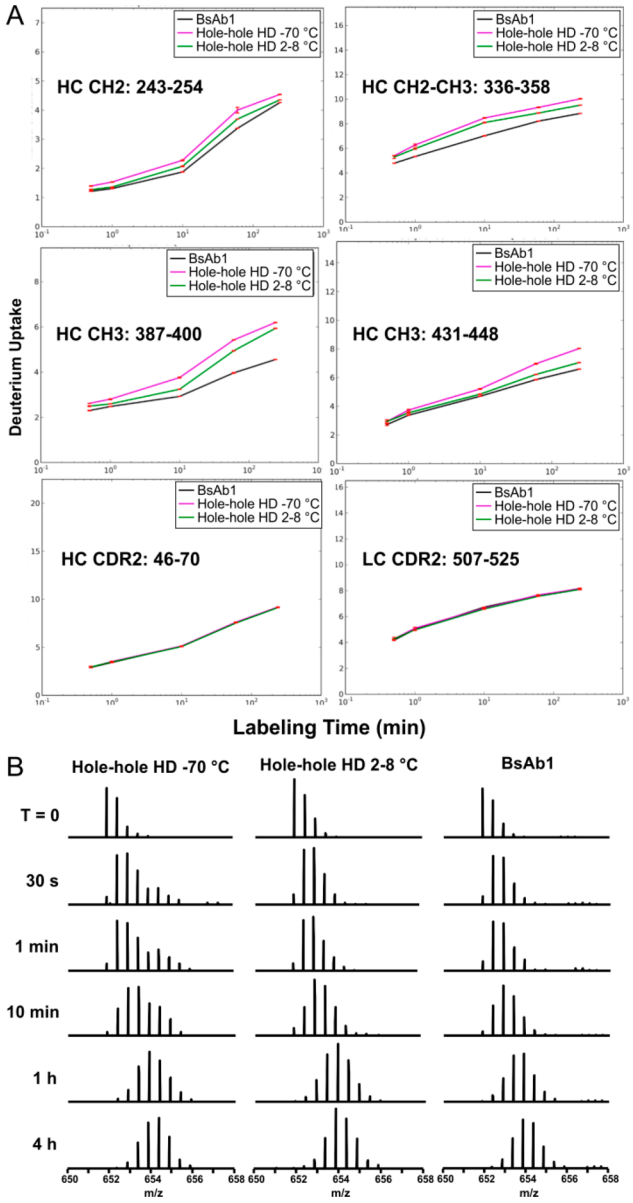

Figure 5. (A) HDX MS time-course results for the hole−hole homodimer (HD) stored at 2−8 °C vs −70 °C compared with BsAb1; (B) Isotopic distribution of a CH2 peptide 243−253 after different periods of deuterium exchange. The −70 °C sample displays EX1 exchange pattern, and the 2−8 °C and BsAb1 samples show EX2 exchange pattern.

Antigen Binding and FcRn Affinity Chromatography of Hole−Hole Homodimer Compared with BsAb1. When characterizing a product-related variant of a biotherapeutic molecule, it is important to understand whether it impacts the function of the molecule. For the BsAb1 molecule, a binding assay was developed (see Supporting Information) to evaluate the antigen binding activity of the hole arm of the BsAb and hole−hole homodimer. Here, this binding assay was used to study the impact of different hole−hole homodimer structural isomers on the antigen binding activity (Figure 6). Since only one arm of the BsAb1 binds to the hole antigen (monovalent binding), BsAb1 should show about 50% binding relative to the homodimers (bivalent). The observed result (53% for BsAb1) demonstrated the capability of this assay to detect relevant differences in hole antigen binding activity. These results

DOI: 10.1021/acs.analchem.7b03830
Anal. Chem. 2017, 89, 13494−13501

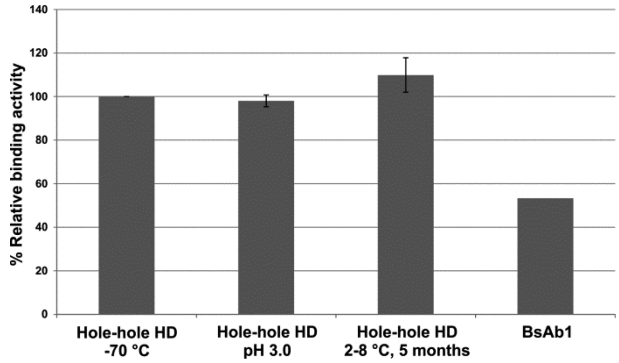

Figure 6. Relative antigen binding of the hole−hole homodimers (HD) in the two storage conditions, −70 °C, 2−8 °C for 5 months and low pH (3.0). BsAb binding was run as a negative control.

indicate that after storage at 2−8 °C for 5 months, or at pH 3.0, even though their HIC profiles show dramatic change, there is little or no difference in antigen binding for the conformational isomers of the hole−hole homodimer. These binding data are consistent with the HDX data showing no changes in Fab structure (Figure 3B).

An FcRn affinity chromatography method was used to evaluate the interaction between FcRn and IgG Fc in vitro, providing insight into the structure that may affect pharmacokinetics (PK) in vivo.[34] As shown in Figure S-3, the BsAb1 displayed a typical FcRn affinity chromatography profile with a single main peak. In contrast, the −70 °C hole−hole homodimer sample showed multiple peaks, one with no FcRn binding affinity, one with low-affinity FcRn binding and one with normal FcRn affinity, whereas the hole−hole homodimer stored at 2−8 °C displayed a main peak and a small peak with low-affinity binding. These results are consistent with the HIC and HDX MS data and correlate well with the structural model shown in Figure 3D. FcRn binds at the interface between the C_H2 and C_H3 domains, and the unfolded Fc (as shown on the left and the middle of the proposed model in Figure 3D at −70 °C) impairs FcRn binding. After storage at 2−8 °C, the Fc conformation changes so as to restore the FcRn binding ability (as shown on the right side of the proposed model in Figure 3D), resulting in a single main peak profile (Figure S-3, middle).

CONCLUSIONS

In this study, we characterized the hole−hole homodimer variant of an in vitro assembled knob-into-hole bispecific antibody by using a suite of analytical and biophysical methods. Multiple conformational isomers were observed in the hole−hole homodimer of BsAb1 by HIC. The more hydrophobic isoforms, as shown by HIC, probably result from partial protein unfolding during the low-pH production process, and these isoforms slowly refold into more compact, less hydrophobic conformation during storage at pH 5.8 and 2−8 °C. High resolution HDX MS identified the location of the conformational change to be at the junction between the C_H2 and C_H3 domains of the hole−hole homodimer. Based on the HDX MS results, we propose that at −70 °C and pH 5.8, the Fc of the hole−hole homodimer is split, forming an X-shaped conformation, as shown by the EM data. After storage at 2−8 °C, the Fc slowly refolds. From the isotopic distribution of the HDX MS data, we also discovered that the hole−hole homodimer stored at −70 °C exhibits heterogeneous conformations, and after storage at 2−8 °C, a homogeneous conformation is generated.

The cause of this unusual conformational change of the hole−hole homodimer during storage at 2−8 °C was discussed. Since the HIC profile displayed reduced hydrophobicity after storage at 2−8 °C, we propose the conformational change during storage is due to the original pH-induced change during purification of the hole−hole homodimer. After it was purified from protein-A chromatography at pH 3.3, an increase to pH 5.8 allowed the hole−hole homodimer to refold from a partially denatured conformation to a more stable and compact conformation very slowly (in the range of weeks when stored at 2−8 °C). This slow conformational change is likely caused by the hole mutations, resulting in disfavored C_H3 dimerization and the slow Fc dimerization/folding.

The bispecific molecule, BsAb1, has the most stable conformation with a homogeneous population, which confirms that the BsAb product are more stable in the purification and storage processes due to the stabilization guided by the knob-into-hole design. We also confirmed that the antigen binding activity of the hole arm of the BsAb and hole−hole homodimer antibody were unchanged, and likewise confirmed that the conformation in the CDRs of the Fab regions were identical by HDX MS. The FcRn affinity chromatography results also confirmed that after storage at 2−8 °C, the Fc of the hole−hole homodimer becomes more folded for better FcRn binding.

The hole−hole homodimer variant is expected to have undesired bioactivity. In addition, the unstable structure of the hole−hole homodimer during storage could pose potential safety or immunogenicity risk to patients. This detailed characterization helps to better understand the product-related hole−hole homodimer variant which could facilitate better monitoring of the variant during production, and ultimately aid in designing safer and more efficacious therapeutic antibodies.

ASSOCIATED CONTENT

Supporting Information

The Supporting Information is available free of charge on the ACS Publications website at DOI: 10.1021/acs.analchem.7b03830.

Methods used for SEC, intact mass analysis by native mass spectrometry, NS EM, the antigen binding assay, and the FcRn affinity chromatography; Figure S-1: HIC profile of the hole−hole homodimers; Figure S-2: SEC for the hole homodimer stored under different conditions and lengths of time; and Figure S-3: FcRn affinity chromatograph for the hole−hole homodimer stored under different conditions and lengths of time (PDF).

AUTHOR INFORMATION

Corresponding Authors

*E-mail: zhang.huimin@gene.com. Tel.: 650-467-9618. Fax: 650-225-3554.

*E-mail: hliu@nektar.com. Tel.: 415-482-5423. Fax: 415-339-5381.

ORCID

Hui-Min Zhang: 0000-0002-2099-4730

Ming Lei: 0000-0002-1247-1358

Present Address

○Nektar Therapeutics, 455 Mission Bay Blvd. South, San Francisco, CA 94158, United States.

DOI: 10.1021/acs.analchem.7b03830
Anal. Chem. 2017, 89, 13494−13501

Author Contributions

All authors have given approval to the final version of the manuscript.

Notes

The authors declare no competing financial interest.

■ ACKNOWLEDGMENTS

The authors would like to thank Ben Walters, Judy Shimoni, and Feng Yang for their critical review of the manuscript; and Yung-Hsiang Kao, John Stults, and John Joly for their support of this project. Work at the Molecular Foundry was supported by the National Science Foundation under Grant DMR-1344290, and the Office of Science, Office of Basic Energy Sciences of the U.S. Department of Energy under Contract No. DE-AC02-05CH11231. D.L. and G.R. were partially supported by the National Heart, Lung, and Blood Institute of the National Institutes of Health (no. R01HL115153) and the National Institute of General Medical Sciences of the National Institutes of Health (no. R01GM104427).

■ REFERENCES

(1) Spiess, C.; Zhai, Q.; Carter, P. J. *Mol. Immunol.* **2015**, *67*, 95−106.
(2) Byrne, H.; Conroy, P. J.; Whisstock, J. C.; O'Kennedy, R. J. *Trends Biotechnol.* **2013**, *31*, 621−632.
(3) Fan, G.; Wang, Z.; Hao, M.; Li, J. *J. Hematol. Oncol.* **2015**, *8*, 130.
(4) Kontermann, R. E.; Brinkmann, U. *Drug Discovery Today* **2015**, *20*, 838−847.
(5) Kontermann, R. E. *BioDrugs* **2009**, *23*, 93−109.
(6) Ridgway, J. B.; Presta, L. G.; Carter, P. *Protein Eng., Des. Sel.* **1996**, *9*, 617−621.
(7) Atwell, S.; Ridgway, J. B.; Wells, J. A.; Carter, P. *J. Mol. Biol.* **1997**, *270*, 26−35.
(8) Spiess, C.; Merchant, M.; Huang, A.; Zheng, Z.; Yang, N. Y.; Peng, J.; Ellerman, D.; Shatz, W.; Reilly, D.; Yansura, D. G.; Scheer, J. M. *Nat. Biotechnol.* **2013**, *31*, 753−758.
(9) Macchi, F. D.; Yang, F.; Li, C.; Wang, C.; Dang, A. N.; Marhoul, J. C.; Zhang, H. M.; Tully, T.; Liu, H.; Yu, X. C.; Michels, D. A. *Anal. Chem.* **2015**, *87*, 10475−10482.
(10) Elliott, J. M.; Ultsch, M.; Lee, J.; Tong, R.; Takeda, K.; Spiess, C.; Eigenbrot, C.; Scheer, J. M. *J. Mol. Biol.* **2014**, *426*, 1947−1957.
(11) Woods, R. J.; Xie, M. H.; Von Kreudenstein, T. S.; Ng, G. Y.; Dixit, S. B. *mAbs* **2013**, *5*, 711−722.
(12) Yin, Y.; Han, G.; Zhou, J.; Dillon, M.; McCarty, L.; Gavino, L.; Ellerman, D.; Spiess, C.; Sandoval, W.; Carter, P. J. *mAbs* **2016**, *8*, 1467−1476.
(13) Strop, P.; Ho, W. H.; Boustany, L. M.; Abdiche, Y. N.; Lindquist, K. C.; Farias, S. E.; Rickert, M.; Appah, C. T.; Pascua, E.; Radcliffe, T.; Sutton, J.; Chaparro-Riggers, J.; Chen, W.; Casas, M. G.; Chin, S. M.; Wong, O. K.; Liu, S. H.; Vergara, G.; Shelton, D.; Rajpal, A.; et al. *J. Mol. Biol.* **2012**, *420*, 204−219.
(14) Wei, H.; Mo, J.; Tao, L.; Russell, R. J.; Tymiak, A. A.; Chen, G.; Iacob, R. E.; Engen, J. R. *Drug Discovery Today* **2014**, *19*, 95−102.
(15) Houde, D.; Arndt, J.; Domeier, W.; Berkowitz, S.; Engen, J. R. *Anal. Chem.* **2009**, *81*, 5966.
(16) Fang, P.; Zhang, H. M.; Shapiro, R.; Marshall, A. G.; Schimmel, P.; Yang, X. L.; Guo, M. *Proc. Natl. Acad. Sci. U. S. A.* **2011**, *108*, 8239−8244.
(17) Xu, X.; Shi, Y.; Zhang, H. M.; Swindell, E. C.; Marshall, A. G.; Guo, M.; Kishi, S.; Yang, X. L. *Nat. Commun.* **2012**, *3*, 681.
(18) Zhang, Q.; Willison, L. N.; Tripathi, P.; Sathe, S. K.; Roux, K. H.; Emmett, M. R.; Blakney, G. T.; Zhang, H. M.; Marshall, A. G. *Anal. Chem.* **2011**, *83*, 7129−7136.
(19) Zhang, A.; Hu, P.; MacGregor, P.; Xue, Y.; Fan, H.; Suchecki, P.; Olszewski, L.; Liu, A. *Anal. Chem.* **2014**, *86*, 3468−3475.
(20) Houde, D.; Peng, Y.; Berkowitz, S. A.; Engen, J. R. *Mol. Cell. Proteomics* **2010**, *9*, 1716−1728.
(21) Zhang, A.; Singh, S. K.; Shirts, M. R.; Kumar, S.; Fernandez, E. J. *Pharm. Res.* **2012**, *29*, 236−250.
(22) Yu, D.; Song, Y.; Huang, R. Y.; Swanson, R. K.; Tan, Z.; Schutsky, E.; Lewandowski, A.; Chen, G.; Li, Z. J. *J. Chromatogr A* **2016**, *1457*, 66−75.
(23) Walters, B. T.; Jensen, P. F.; Larraillet, V.; Lin, K.; Patapoff, T.; Schlothauer, T.; Rand, K. D.; Zhang, J. *J. Biol. Chem.* **2016**, *291*, 1817−1825.
(24) Pan, L. Y.; Salas-Solano, O.; Valliere-Douglass, J. F. *Anal. Chem.* **2014**, *86*, 2657−2664.
(25) Zhang, L.; Ren, G. *J. Phys. Chem. Biophys* **2012**, *2*, No. e103, DOI: 10.4172/2161-0398.1000e103.
(26) Kan, Z. Y.; Mayne, L.; Chetty, P. S.; Englander, S. W. *J. Am. Soc. Mass Spectrom.* **2011**, *22*, 1906−1915.
(27) Wales, B. T. *Ph.D. Thesis*, University of Pennsylvania, ProQuest Dissertation Publishing, 2013; pp 71−79.
(28) Hall, Z.; Robinson, C. V. *J. Am. Soc. Mass Spectrom.* **2012**, *23*, 1161−1168.
(29) Smith, D. L.; Deng, Y.; Zhang, Z. *J. Mass Spectrom.* **1997**, *32*, 135−146.
(30) Cravello, L.; Lascoux, D.; Forest, E. *Rapid Commun. Mass Spectrom.* **2003**, *17*, 2387−2393.
(31) Zhang, H. M.; Kazazic, S.; Schaub, T. M.; Tipton, J. D.; Emmett, M. R.; Marshall, A. G. *Anal. Chem.* **2008**, *80*, 9034−9041.
(32) Weis, D. D.; Wales, T. E.; Engen, J. R.; Hotchko, M.; Ten Eyck, L. F. *J. Am. Soc. Mass Spectrom.* **2006**, *17*, 1498−1509.
(33) Zhang, H. M.; Yu, X.; Greig, M. J.; Gajiwala, K. S.; Wu, J. C.; Diehl, W.; Lunney, E. A.; Emmett, M. R.; Marshall, A. G. *Protein science: a publication of the Protein Society* **2010**, *19*, 703−715.
(34) Schlothauer, T.; Rueger, P.; Stracke, J. O.; Hertenberger, H.; Fingas, F.; Kling, L.; Emrich, T.; Drabner, G.; Seeber, S.; Auer, J.; Koch, S.; Papadimitriou, A. *mAbs* **2013**, *5*, 576−586.

DOI: 10.1021/acs.analchem.7b03830
Anal. Chem. 2017, 89, 13494−13501

Supporting Information

Structural and Functional Characterization of a Hole-Hole Homodimer Variant in a "Knob-Into-Hole" Bispecific Antibody

Hui-Min Zhang,*,† Charlene Li,† Ming Lei,† Victor Lundin,† Ho Young Lee,‡ Milady Ninonuevo,† Kevin Lin,ǀ Guanghui Han,§ Wendy Sandoval,§ Dongsheng Lei,‖ Gary Ren,‖ Jennifer Zhang,† and Hongbin Liu*,†‡

† Protein Analytical Chemistry, Genentech Inc., 1 DNA Way, South San Francisco, California 94080, United States
‡ Biological Technologies, Genentech Inc., 1 DNA Way, South San Francisco, CA 94080, United States
ǀ Analytical Operations, Genentech Inc., 1 DNA Way, South San Francisco, CA 94080, United States
§ Departments of Microchemistry, Proteomics and Lipidomics, 1 DNA Way, South San Francisco, CA 94080, United States
‖ The Molecular Foundry, Lawrence Berkeley National Laboratory, One Cyclotron Road, Berkeley, CA 94720, United States
‡ Current address: Nektar Therapeutics, 455 Mission Bay Blvd. South, San Francisco, CA 94158

* Corresponding Authors. H.-M. Zhang E-mail: zhang.huimin@gene.com Tel: 650-467-9618, Fax: 650-225-3554 or H. Liu E-mail: hliu@nektar.com, Tel: 415-482-5423, Fax: 415-339-5381

This supporting information provides a detailed description of the materials and methods used for size-exclusion chromatography, native MS, negative-staining electron microscopy, the antigen binding assay to measure the binding of hole HD with the antigen peptide, AND.

Contents

Size Exclusion Chromatography

SEC was performed on an Agilent 1200 HPLC (Agilent Technologies, Santa Clara, CA) with a TSK G3000SW$_{XL}$ column, 7.8 × 300 mm (Tosoh Biosciences, King of Prussia, PA). The mobile phase was 0.2 M potassium phosphate buffer (pH 6.2) containing 0.25 M potassium chloride. Each sample was diluted to 1 mg/mL with the mobile phase. The protein load for each injection was 50 µg. The separation was conducted at ambient temperature with a flow rate of 0.5 mL/min. The column effluent was monitored at 280 nm UV wavelength.

Intact Mass Analysis by Native Mass Spectrometry

For the native MS experiment, 25–50 µg of the hole-hole homodimer samples were buffer-exchanged using Micro Bio-Spin TM 6 columns, prepackaged in Tris buffer (Bio-Rad Laboratories, Inc., Hercules, CA). The column was first centrifuged at 3300 rpm at 4 °C to flush the Tris buffer and then rinsed five times in 100 mM ammonium acetate (Sigma-Aldrich Corp., St. Louis, MO) by loading the column with 0.5 mL of buffer and centrifuging for 1 min at 3300 rpm at 4 °C. The collection tube was emptied after each spin. The column was then placed in a new collection Eppendorf tube, and 25–50 µg of sample were added on the resin at the center of the column. The column was then centrifuged for 10 min at 2000 rpm at 4 °C. The buffer-exchanged sample was collected in the Eppendorf tubes.

Samples were directly infused into an Exactive Plus extended mass range (EMR) Orbitrap mass spectrometer (Thermo Scientific, San Jose, CA) via nanospray ionization using a Triversa TM Nanomate (Advion, Inc., Ithaca, NY). The instrument was set in EMR MS mode for intact mass analysis. The IgG samples were analyzed under the following acquisition parameters: spray gas pressure, 1.0 psi; spray voltage, 1.50 kV; Capillary temperature, 250 °C; S-lens RF level, 100; Scan rage, 1000 to 10000 m/z; Desolvation, in-source CID 120 ev, collision energy, 0; Resolution, 17500 at m/z 200; Polarity, positive; Microscans, 10; AGC targe, 3e6; Maximum injection time, 50; Averaging, 100; Source DC offset, 25V; Injection Flatapole DC, 8V; Inter Flatapole lens, 7V; Bent Flatapole DC, 6V; Transfer multipole DC tune offset, 0V; C-Trap entrance lens tune offset, 0V; Trapping gas pressure setting, 5. Spectra were visualized using Thermo Xcalibur Qual Browser then annotated manually. Mass spectrometric data was analyzed using Protein Deconvolution v4.0 software (Thermo Scientific).

Negative-Staining Electron Microscopy (NS EM)

Conventional cryo-electron microscopy (cryo-EM) is often the method of choice for studies of protein structure under physiological conditions because it avoids potential artifacts from fixatives and stains.[1] Still, cryo-EM studies of antibodies are challenging due to their small molecular mass (~150 kDa) and flexible structure.[2] Thus, we used an

optimized negative-staining (OpNS) protocol,[1,3] which was refined from the conventional negative staining protocol by using cryo-EM images as a control. OpNS EM images present a much higher image contrast than cryo-EM images with a reasonable resolution (1–3 nm) for visualizing the domains of each antibody. OpNS has been used to examine many proteins, such as antibodies,[4,5] GroEL,[6] and Glycyl-tRNA synthetase.[7] Through those studies OpNS has been validated as a general protocol.

The negative-staining specimens of antibody homodimers were prepared by using optimized negative-staining (OpNS) protocol as described previously.[1,3] Briefly, antibody samples were diluted to ~ 0.04 μg mL^{-1} with Dulbecco's phosphate buffered saline (DPBS). An aliquot (~ 4 μL) of diluted sample was then placed on an ultra-thin carbon-coated 200-mesh copper grid (CF200-Cu-UL, Electron Microscopy Sciences, Hatfield, PA, USA) that had been glow-discharged for 15 s. After 1 min incubation, the excess solution on grid was blotted with filter paper. The grid was then washed with water and stained with 1% (w/v) uranyl formate (pH ~4.5) before air-drying with nitrogen.[1,3]

Samples were examined by using a Zeiss Libra 120 Plus TEM (Carl Zeiss NTS) operated at 120 kV high tension. The micrographs were acquired under defocus between ~0.6 μm and ~0.9 μm. A dose of ~40-90 $e^-/Å^2$ using a Gatan UltraScan 4K X 4K CCD under a magnification of 80 kx (each pixel of the micrographs corresponds to 1.48 Å in specimens) was used. The contrast transfer function (CTF) of each micrograph was examined by ctffind3[8] and corrected by use of the SPIDER[9] software after the X-ray speckles were removed. Particles were then selected from the micrograph with a box size of 256 × 256 by use of boxer (EMAN[10] software). All particles were masked by a round mask generated from SPIDER after a Gaussian high-pass filtering. The reference-free class averages of particles were obtained by using refine2d (EMAN software) based on 2631 particles for the antibody sample stored at -70˚C.

Crystal structure of mouse IgG2 antibody (PDB entry 1IGT[11]) was superimposed on representative images of particles (Y- and X-shapes) to reflect the structural dynamics of the hole-hole homodimer. The two F_{ab} domains and two chains of F_c domains within 1IGT were rigid-body rotated and translated to obtain their best superimposition onto the representative particle images using Chimera.[12]

Antigen Binding Assay to Measure the Binding of Hole Homodimer with the Antigen Peptide

A 96-well high binding polystylen microtiter plate was incubated for 16-72 h at 4 °C with 100 μL of 3 μg/mL of Neutravidin in DPBS (-$Ca^{2+,}$ -Mg^{2+}). The plate was washed with wash buffer (1x PBS, pH 7.4, 0.05% Polysorbate 20) twice with auto program (6 times wash) using a BioTek 405 plate washer. The plate was blocked with 200 μL of blocking buffer (1x PBS, pH 7.4, 0.05% Polysorbate 20, 0.5% BSA) at 25 °C for 1-2 h. Then the plate was washed as above. 100 μL of biotinylated antigen peptide (2 μg/mL) in assay diluent (1x PBS, 0.05% Polysorbate 20, 0.5% BSA) was added to each well, and incubated at 25 °C for 1 h. While incubating the plate, experimental samples were diluted accordingly using assay diluent. After incubation with the antigen peptide, the plate was washed as described above, and 100 μL of the sample diluents were added to the plate. The sample diluents were incubated at 25 °C for 1 h. After washing, 100 μL of 3 ng/mL of goat anti-human-IgG (Fab')2 HRP (Jackson ImmunoResearch

Cat.No.109-036-097) in assay diluent was added and incubated at 25 °C for 1 h. The plate was washed after the incubation, and 100 µL of TMB substrate (SureBlue Reserve TMB Microwell Poroxidase substrate, KPL, cat. No. 53-00) was added and incubated until the color developed adequately. 100 µL of 0.6N sulfuric was added to quench the reaction. The plate was measured for the optical density (OD) values on the plate reader using two wavelengths, 450 nm for detection absorbance and 650 nm for reference absorbance. The data were analyzed with SoftMaxPro software by 4P analysis, and relative potency was calculated using the -70 °C hole homodimer as standard.

FcRn Affinity Chromatography to Evaluate the Hole-hole Homodimer's Fc Structural Integrity

FcRn affinity chromatography was performed on Thermo/Dionex Ultimate 3000 UHPLC system. The soluble extracellular domain of FcRn with His-Avi-Tag® associated with beta-2-microglubulin was immobilized onto POROS® streptavidin beads that were packed into a 300 µL column[13]. Mobile phase A was 20 mM MES(2-(N-morpholino)ethanesulfonic acid , 150 mM NaCl, pH 6.0, mobile phase B was 20 mM MES, 150 mM NaCl, pH 6.5 and mobile phase C was 20 mM Tris/HCl, 150 mM NaCl, pH 8.5. The flow rate was 0.25 mL/min. Samples were diluted to 1.0 mg/mL in mobile phase A. Approximately 30 µg of each sample was loaded onto the column, where it was eluted using the following pH gradient: 100% mobile phase A to 66% mobile phase B in 5 minutes; to 75 % B and 25% C in 5 minutes; to 15% B and 75% C in 20 minutes; to 100% C in 8 minutes; hold 100% C for 9 minutes; to 100% A in 2 minutes; hold 100% A for 12 minutes. The elution was monitored by UV absorption at 280 nm, and the pH was monitored using an on-line pH meter.

Figure S-1. Hydrophobic interaction chromatography (HIC) profile of the hole-hole homodimers

Hole-hole homodimer (HD) at different time points during storage at 2-8 °C, after buffer exchange to pH 7.5 from the first buffer exchange (pH 5.8 to pH 3.0) for 1.5, 3 and 18 h, compared with the hole-hole HD frozen control. (Note: the -70 °C controls were made from different batches, so the frozen control here is different from the ones in Figure 1.)

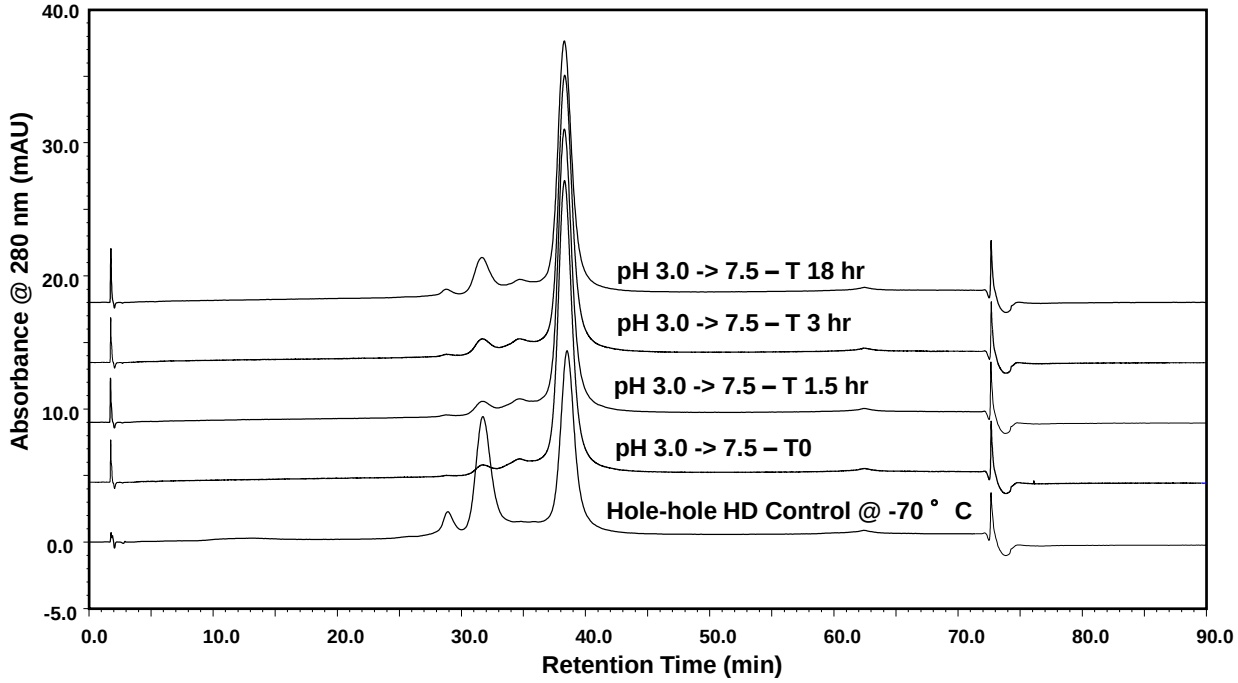

Figure S-2. SEC for the hole-hole homodimer (HD) stored under different conditions and lengths of time (The insert is the overlay).

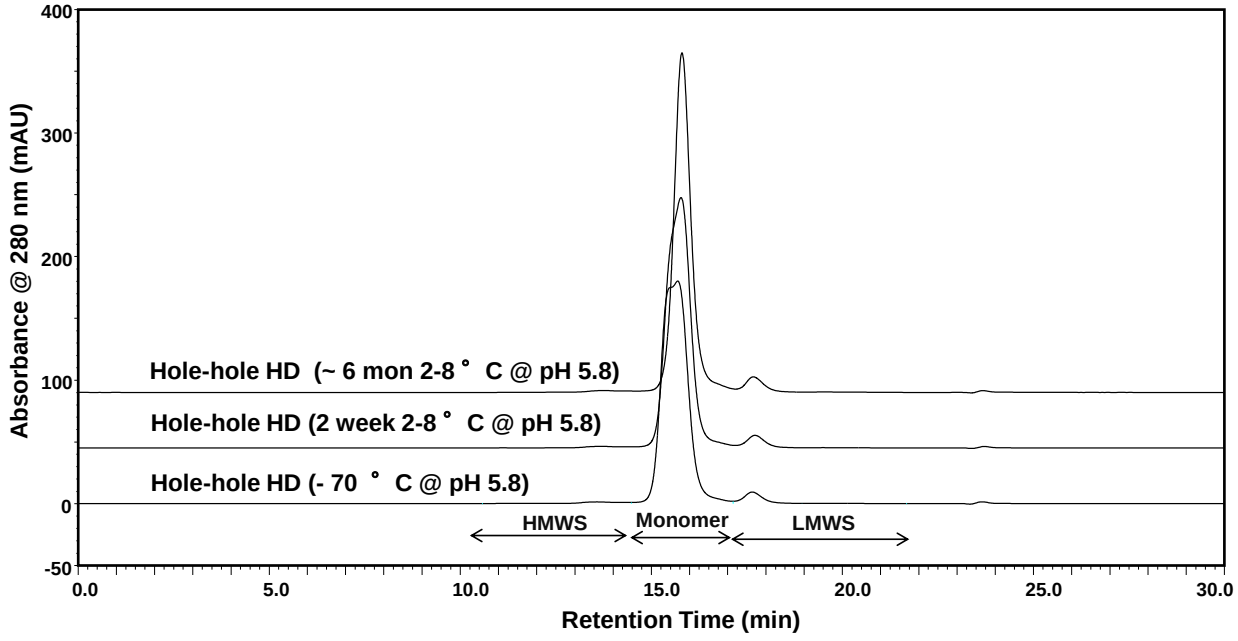

Figure S-3. FcRn Affinity Chromatography for the hole-hole homodimer (HD) stored at -70 °C and 2-8 °C, as well as the BsAb1 samples.

The hole-hole HD stored at -70 °C displayed three peaks, a flow-through peak (no binding), a low-affinity binding peak, and a main peak. The hole-hole HD stored at 2-8 °C displayed a main peak and a small peak with low-affinity binding. The BsAb1 displayed a single main peak. Note that the retention time is slightly different between the bispecific antibody and the hole-hole HD at 2-8 °C, possibly due to their slightly different Fc structure.

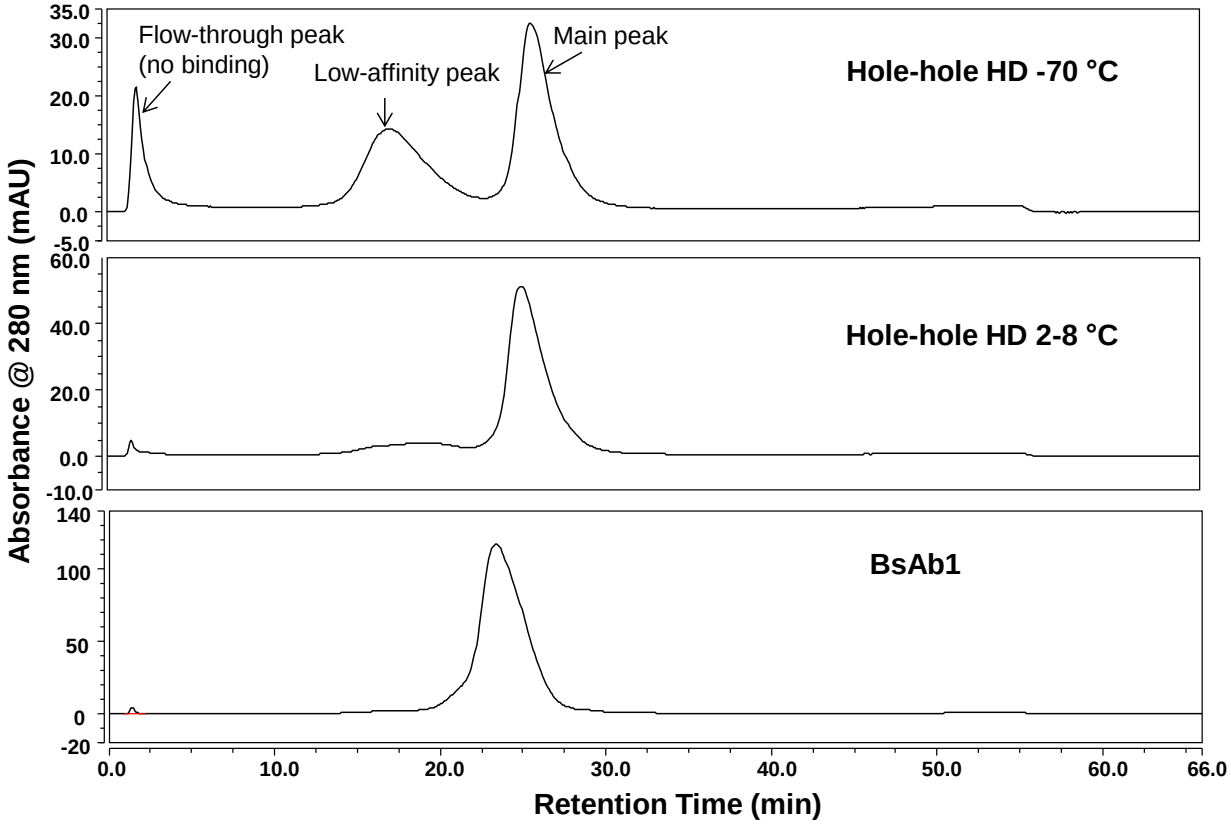

REFERENCES

(1) Zhang, L.; Song, J.; Newhouse, Y.; Zhang, S.; Weisgraber, K. H.; Ren, G. *Journal of lipid research* **2010**, *51*, 1228-1236.
(2) Ohi, M.; Li, Y.; Cheng, Y.; Walz, T. *Biol Proced Online* **2004**, *6*, 23-34.
(3) Zhang, L.; Song, J.; Cavigiolio, G.; Ishida, B. Y.; Zhang, S.; Kane, J. P.; Weisgraber, K. H.; Oda, M. N.; Rye, K. A.; Pownall, H. J.; Ren, G. *Journal of lipid research* **2011**, *52*, 175-184.
(4) Zhang, X.; Zhang, L.; Tong, H.; Peng, B.; Rames, M. J.; Zhang, S.; Ren, G. *Sci Rep* **2015**, *5*, 9803.

(5) Zhang, L.; Tong, H.; Garewal, M.; Ren, G. *Biochim Biophys Acta* **2013**, *1830*, 2150-2159.
(6) Rames, M.; Yu, Y.; Ren, G. *J. Vis. Exp.* **2014**, e51087.
(7) Deng, X.; Qin, X.; Chen, L.; Jia, Q.; Zhang, Y.; Zhang, Z.; Lei, D.; Ren, G.; Zhou, Z.; Wang, Z.; Li, Q.; Xie, W. *J Biol Chem* **2016**, *291*, 5740-5752.
(8) Mindell, J. A.; Grigorieff, N. *Journal of structural biology* **2003**, *142*, 334-347.
(9) Frank, J.; Radermacher, M.; Penczek, P.; Zhu, J.; Li, Y.; Ladjadj, M.; Leith, A. *Journal of structural biology* **1996**, *116*, 190-199.
(10) Ludtke, S. J.; Baldwin, P. R.; Chiu, W. *Journal of structural biology* **1999**, *128*, 82-97.
(11) Harris, L. J.; Larson, S. B.; Hasel, K. W.; McPherson, A. *Biochemistry-Us* **1997**, *36*, 1581-1597.
(12) Pettersen, E. F.; Goddard, T. D.; Huang, C. C.; Couch, G. S.; Greenblatt, D. M.; Meng, E. C.; Ferrin, T. E. *J Comput Chem* **2004**, *25*, 1605-1612.
(13) Schlothauer, T.; Rueger, P.; Stracke, J. O.; Hertenberger, H.; Fingas, F.; Kling, L.; Emrich, T.; Drabner, G.; Seeber, S.; Auer, J.; Koch, S.; Papadimitriou, A. *mAbs* **2013**, *5*, 576-586.